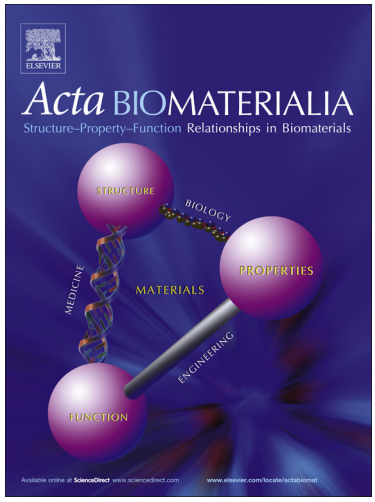

Full length article

Ultrastructural organization of elastic fibres in the partition boundaries of the annulus fibrosus within the intervertebral disc

J. Tavakoli, J.J. Costi

PII: S1742-7061(17)30783-3
DOI: https://doi.org/10.1016/j.actbio.2017.12.017
Reference: ACTBIO 5229

To appear in: *Acta Biomaterialia*

Received Date: 18 August 2017
Revised Date: 14 December 2017
Accepted Date: 14 December 2017

Please cite this article as: Tavakoli, J., Costi, J.J., Ultrastructural organization of elastic fibres in the partition boundaries of the annulus fibrosus within the intervertebral disc, *Acta Biomaterialia* (2017), doi: https://doi.org/10.1016/j.actbio.2017.12.017

Ultrastructural organization of elastic fibres in the partition boundaries of the annulus fibrosus within the intervertebral disc

Tavakoli J,[1] Costi JJ[1]

[1]Biomechanics and Implants Research Group, The Medical Device Research Institute, College of Science and Engineering, Flinders University, GPO Box 2100, Adelaide, South Australia 5001, Australia

*Corresponding author: John J. Costi, john.costi@flinders.edu.au

Abstract

The relationship between elastic fibre disorders and disc degeneration, aging and progression of spine deformity have been discussed in a small number of studies. However, the clinical relevance of elastic fibres in the annulus fibrosus (AF) of the disc is poorly understood. Ultrastructural visualization of elastic fibres is an important step towards understanding their structure-function relationship. In our previous studies, a novel technique for visualization of elastic fibres across the AF was presented and their ultrastructural organization in intra- and inter-lamellar regions was compared. Using the same novel technique in the present study, the ultrastructural organization of elastic fibres in the partition boundaries (PBs), which are located between adjacent collagen bundles, is presented for the first time. Visualization of elastic fibres in the PBs in control and partially digested (digested) samples was compared, and their orientation in two different cutting planes (transverse and oblique) were discussed. The ultrastructural analysis revealed that elastic fibres in PBs were a well-organized dense and complex network having different size and shape. Adjacent collagen bundles in a cross section (CS) lamella appear to be connected to each other, where elastic fibres in the PBs were merged in parallel or penetrated into the collagen bundles. There was no significant difference in directional coherency coefficient of elastic fibres between the two different cutting planes ($p = 0.35$). The present study revealed that a continous network of elastic fibres may provide disc integrity by connecting adjacent bundles of CS lamellae together. Compared to our previous studies, the density of the elastic fibre network in PBs was lower, and fibre orientation was similar to the intra-lamellar space and inter-lamellar matrix.

Keywords: Partition boundaries, Elastic fibres, Ultrastructural organization, Annulus fibrosus, Fibre orientation

1. Introduction

Elastic fibres are critical components of the extracellular matrix in biological structures, whose defects affect tissue elasticity and contribute to pathologies (e.g. cutis laxa, Williams-Beuren syndrome, scoliotic discs, etc.) degeneration and aging [1-4]. The role of elastic fibres in the intervertebral disc is not clearly understood, although few studies revealed their contribution to radial integrity of the annulus fibrosus (AF) [5-7]. On the other hand, the relationship between elastic fibre disorders and disc degeneration suggests that more structure-function studies need to be performed to identify the impact of elastic fibres on disc mechanical properties [8-12]. A clinical observation found that compared to healthy discs, scoliotic discs have a disorganized and sparse elastic network, which could contribute to the progression of spine deformity [8]. It was demonstrated that with increasing age and disc degeneration, elastic fibre morphology appears to become more disorganized [9]. In addition, an increase of metalloproteinase level in scoliotic discs leads to elastin degradation [10, 11] as well as activation of elastase enzymes in degenerated discs [12].

Early efforts to establish the presence of elastic fibres as an organizational constituent of the disc using Scanning Electron Microscopy (SEM) were unsuccessful [13, 14]; however, they were observed by Buckwalter et al. in 1976 [15]. Several other investigators confirmed the presence of elastic fibres in the disc; however, their observations did not reveal elastic fibre ultrastructure [16-19]. Based on low elastin content [20-22], and its irregular distribution across the disc, elastic fibres were thought to play no role in disc function [23]. However, a light microscopy study revealed that there was an abundant elastic fibre network distributed across all regions of the disc [24]. Elastic fibres were found to be comprised of a central elastin core component integrated with the surrounding fibrillin framework [25], after which it was revealed that both elastin and fibrillin were extensively distributed across the AF [26].

This understanding has been developed through other studies to highlight the potential role of elastic fibres on disc structural and mechanical properties [20, 23, 27-29].

Early microstructural investigation indicated that elastic fibres have different oblique and longitudinal orientations within the AF [30] and are more dense in the outer compared to the inner AF [31]. Dissimilarity of the AF elastic fibre density in circumferential and radial locations was also explained in a microscopic study [27]. At the light microscopy scale (20× magnification), it was discovered that the long elastic fibres of the nucleus pulposus extend radially towards the AF, while some were oriented towards the endplates [23, 24]. Also it was found that elastic fibres of the AF appeared to be aligned parallel to the collagen fibres within the lamellae [24, 26, 28] and were more dense and of complex arrangement in the inter-lamellar matrix (ILM) [24, 26, 28, 32]. A study showed that elastic fibres enhanced the AF lamellae interconnectivity, while surrounding collagen bundles [33]. This study revealed that collagen bundles in a cross section (CS) lamella are subdivided by a dense structure of elastic fibres, a region identified as a partition boundary (PB), which may divide the entire lamella or appears as incomplete dividers [33]. The PBs were more likely to be seen in CS, rather than in-plane lamellae (IP) [33]. Identification of CS and IP lamellae depends on the cutting plane and has been defined elsewhere [34, 35]. Briefly, collagen bundles in oblique sections are parallel in an IP lamellae, and perpendicular to the cutting plane in a CS lamella.

Although these light microscopic studies showed that elastic fibres were found throughout the AF within three different regions including intra-lamellar, ILM and PB, none were able to provide the fine-scale and ultra-architectural details of the elastic fibre network. On the other hand, since all fibrous elements including collagen and elastic fibres, are intermingled with each other and masked by the matrix, their ultra-structural organization was not possible to be visualised under low (light microscopic level), nor at higher magnifications (SEM).

Visualization of the AF elastic fibre ultrastructural organization in intra-lamellar region and the ILM has recently been achieved using a novel technique incorporating sodium hydroxide-sonication digestion followed by heat treatment [36]. However, less is known about elastic fibres ultrastructural organization within the PBs. It was demonstrated that large parallel elastic fibres were connected to each other by very fine elastic fibres and form a loose network within the intra-lamellar region. An ultrastructural study of elastic fibres revealed that a dense and complex network, including thick (approximately 1-2 µm in diameter) and thin (0.1 µm diameter) elastic fibres, exist in the ILM [37]. It was demonstrated that interconnecting elastic fibres in the ILM were not organized randomly, which supports the hypothesis that they may be involved in distributing stresses through the AF, while enhancing its structural integrity. Based on the literature review, there is evidence that elastic fibres, having a complex pattern of interconnectivity, exist in three main regions of the AF (Table 1).

Table 1- Three main regions where elastic fibre structural characteristics were described under low (light microscopy) and high (SEM) magnifications.

Region	Location	Structural characteristics
Intra-lamellar	Within the lamella	*Low magnification:* Long elastic fibres are in parallel to the collagen fibres [5, 8, 20, 24]. *High magnification:* A loose network (not randomly distributed) of elastic fibres was observed in the intra-lamellar region, which are comprised of thick fibres aligned parallel to the collagen fibres (0.3-0.5 µm diameter), and very fine interconnecting fibres of less than 0.3 µm diameter [37].
Inter-lamellar (ILM)	Between adjacent lamellae	*Low magnification:* A complex and dense structure was present in the ILM [8, 24, 26, 27, 32]. *High magnification:* A dense network including thick (diameter of 1-2 µm) and thin (0.1 µm diameter) elastic fibres was seen in the ILM. This complex network was not randomly distributed, consisting of different size and shape fibres, differs to those located in the intra-lamellar region [37].
Partition Boundaries (PB)	Between collagen bundles	*Low magnification:* Elastic fibres are the main component of the PB [33]. *High magnification:* No study was performed.

Investigation of the ultrastructural organization of elastic fibres within the PBs will help to improve the knowledge of the AF elastic fibre interconnectivity within the ILM, PB and intra-lamellar regions. Understanding the ultrastructural organization of elastic fibres in PBs will support further studies on the AF structure-function properties, the role of elastic fibres on herniation, and their impact on mechanical behaviour of the disc. In addition, elastic fibre ultrastructural analysis can be utilized to develop a 3D map of disc elastic fibre distribution to design tissue engineered scaffolds for AF repair and replacement.

Therefore, the aims of this study were: first to present an ultra-structural analysis of the elastic fibre network in the PBs of the AF using Scanning Electron Microscopy (SEM); and second, to investigate whether the elastic fibre orientation and distribution within the PBs change when viewed from two different cutting planes.

2. Materials and methods

2.1. Sample preparation

Discs (level L1/2) from nine lumbar sheep spines (2 years old) were obtained from a local abattoir, dissected from vertebral bodies, sprayed with saline and stored at -20°C until used for sample preparation. While frozen, a 10 mm length of the anterior AF was separated from each disc and were cut into half, transversally (Figures 1a, a-1 and a-2) to obtain two groups of nine tissue sections. Both tissue section groups were mounted with optimal cutting temperature compound (O.C.T, Tissue-Tek®) at two angles of approximately 0° and 30° to the transverse plane to identify the cutting planes, respectively (Figures 1b and 1c). From each of the eighteen tissue sections, samples from adjacent sections (30 µm thickness) were cut using a cryostat microtome (Leica Biosystems, CM3050) in oblique (Figure 1d) and

transverse (Figure 1e) cutting angles. Control (undigested) and digested samples were prepared for elastic fibre visualization through scanning electron microscopy [36, 37].

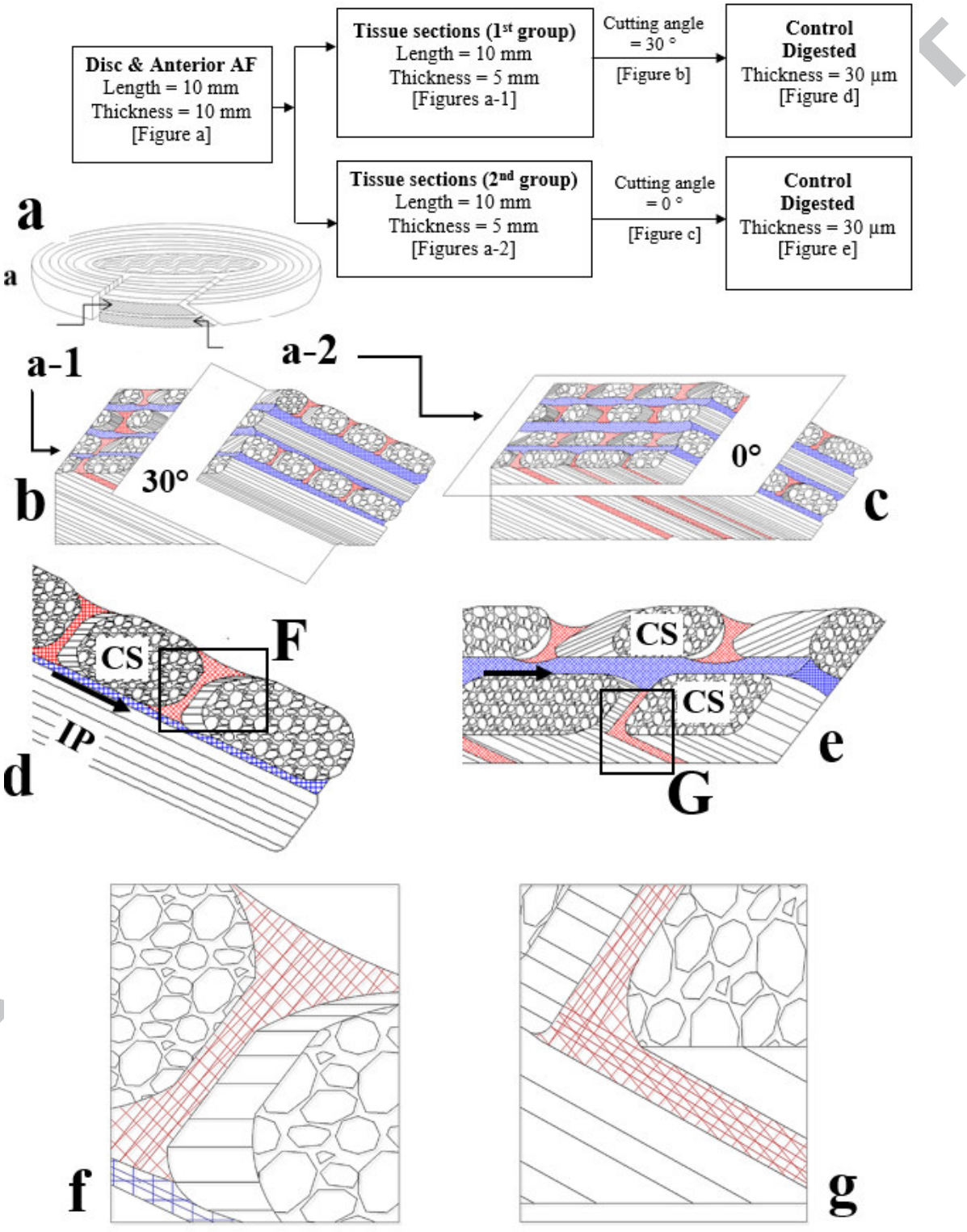

Figure 1. Sample preparation methodology and schematic drawing. Anterior AF strips (10 mm in length) were separated from the disc and were cut into half, transversally (a). Frozen sections prepared at two angles of approximately 30° (oblique cut, b) and 0° (transverse cut, c) relative to the transverse axis. Zoomed-in schematic drawings of two adjacent lamellae of samples that were cut by microtome to a thickness of 30 µm along the cutting planes are shown (d, e) and can be utilized to identify different anatomic locations of PBs (red shaded lines) relative to the ILM (blue). F and G boxes represent magnified regions as shown in f and g images, respectively, to identify the orientation of elastic fibres in the PBs. PBs connect collagen bundles together, while the ILM provides cohesion strength between adjacent lamellae (d, e). The TCD axis is shown at both transverse and oblique cutting planes by black arrows (d, e).

2.2. Sample digestion

NaOH partially digestion (digestion) was performed in accordance with a novel technique incorporating sodium hydroxide-sonication digestion followed by heat treatment to prepare the AF samples for ultrastructure visualization of elastic fibres using SEM [36]. Briefly, samples were sonicated in 0.5 M sodium hydroxide solution (SONIC-950WT, MRC, Germany) at 37℃ for 25 min and then washed in distilled water. An indirect heating treatment using a water bath at 70 ℃ for 5 min was performed to remove collagen fibres, leaving the elastic network intact (digested sample). Digested samples were dried in a vacuum oven (VO3, LABEC, Australia) at 37℃ and -80 kPa overnight for SEM investigation.

2.3. Scanning electron microscopy

Using double adhesive tape, samples were mounted on aluminium stubs and sputter coated (EmiTech K575X) with platinum at 2 nm thickness. A high voltage of 5 kV was set for SEM

imaging (Inspect F50, FEI Company, USA). SEM images were acquired from the sample surface, while the distance from the sample to the beam source was kept constant. For SEM imaging the samples were scanned at high magnification first (<50 µm) since elastic fibres were not visible at low magnifications (>200 µm). Once elastic fibres in the digested region were identified, a low magnification was used as a starting point from which sequential images were acquired at the region of interest at progressively increasing magnifications.

2.4. Quantitative analysis

SEMs of elastic network in the PBs were used to assess the degree of elastic fibre alignment relative to the tangent to the circumferential direction (TCD plane), which passes vertically through the ILM (Figures 1d, 1e and 7-b), using an open source software (ImageJ) [38]. All SEM images were manually edited to remove non-elastin components, using a graphics editor software (paint.NET for Microsoft Windows, v3.5.10, Rick Brewster, dotPDN LLC) utilizing Magic wand editing option and selecting a 15% tolerance. The manual editing technique and its effect on coherency coefficient values was evaluated by conducting an intra-rater repeatability analysis. SEM images were randomly selected from five out of the nine specimens from each of the oblique and transverse samples. The manual editing technique was repeated 3 times each, giving a total of 30 sample images. The OrientationJ plugin was used to measure the directional coherency coefficient of elastic fibres in the input 8 bit images, utilizing a pre-filter option with the Laplacian of Gaussian (Sigma) equal to zero. Fibre count-orientation analysis was conducted in the binary images with Cubic Spline Gradient selected as the structural tensor for fitting the data [38- 39].

2.5. Statistical analysis

An independent samples t-test was conducted (IBM SPSS Statistics for Windows, Version 22.0. Armonk, NY: IBM Corp.), having a test variable of directional coherency coefficient of

elastic fibres within the PBs between two different cutting plane angles (transverse and oblique) using an alpha of 0.05. To assess intra-rater repeatability of the manual image editing technique for measuring directional coherency coefficients, an Intra-class Correlation Coefficient (ICC) for reliability was conducted, as described by Koo and Li [40].

3. Results

3.1. Comparing control and digested samples

To clarify the effect of digestion, a comparison between control and digested samples was performed. Figure 2 presents the SEM images of the PB at different magnifications for both control (Figures 2a-b) and digested samples in oblique (Figures 2c-d) and transverse (Figures 2e-f) cutting planes. The PBs, located between collagen bundles, divide the AF collagenous compartment (collagen bundles) irregularly and alternately, while running through the lamella. As shown in Figures 2a and 2b, these PB structures (some denoted by stars) can be distinguished more readily in the CS lamellae containing collagen bundle cross sections rather than those having parallel collagen fibres (IP lamellae). However, identification of their ultrastructural organization wasn't possible at high and low magnifications for control samples using SEM imaging (Figures 2a-b) since all intermingled fibres were obscured by the matrix. At 100 µm scale bar (1702×) in a control sample (Figure 2b), almost parallel traversing PBs in the CS lamellae seemed to separate collagen bundle compartments.

As shown in Figures 2c-f, removing proteoglycans together with a significant decrease in matrix masking effect led to a better visualization of the PBs at both cutting angles, oblique (Figures 2c-d) and parallel (Figures 2e-f) to the transverse plane. Gradual removal of matrix that occurred as a result of digestion, revealed a progressive improvement in visualization of fibres within the CS compared to the IP lamellae in all samples. It appeared that a CS lamella experienced faster digestion compared to the IP, where tightly packed parallel collagen fibres

were presented. Following the digestion of the AF matrix, organization of collagen bundles in a CS lamellae was observed in an oblique cutting plane (30°). In a CS lamella, collagen bundles that were covered by remnants of undigested matrix were perpendicular to the sample surface (a typical bundle cross section denoted by dashed lines in figure 2d) whose collage fibres ran inward (denoted by arrow).

Digestion of adjacent lamellae in a transverse cutting plane (0°) facilitated the organization of PBs to be visualized (denoted by stars in Figures 2f). Compared to the control (undigested) samples digestion clarified how PBs might run between adjacent lamellae, while connecting them together (Figure 2f). Referring to control samples, it was hard to see whether collagen bundles were divided completely by PBs. However, in digested samples (Figures 2e and f), it was apparent that the size, orientation and pattern of PBs were irregular and they frequently divided the entire CS lamella or connected to other PBs, while linking adjacent lamellae. The compartmentalization of the entire lamella seems to result in creating a fenestration across all adjacent CS lamellae. Large fenestrae, shown by arrow heads in Figure 2f, were introduced after orthogonal collagen bundles were removed following digestion.

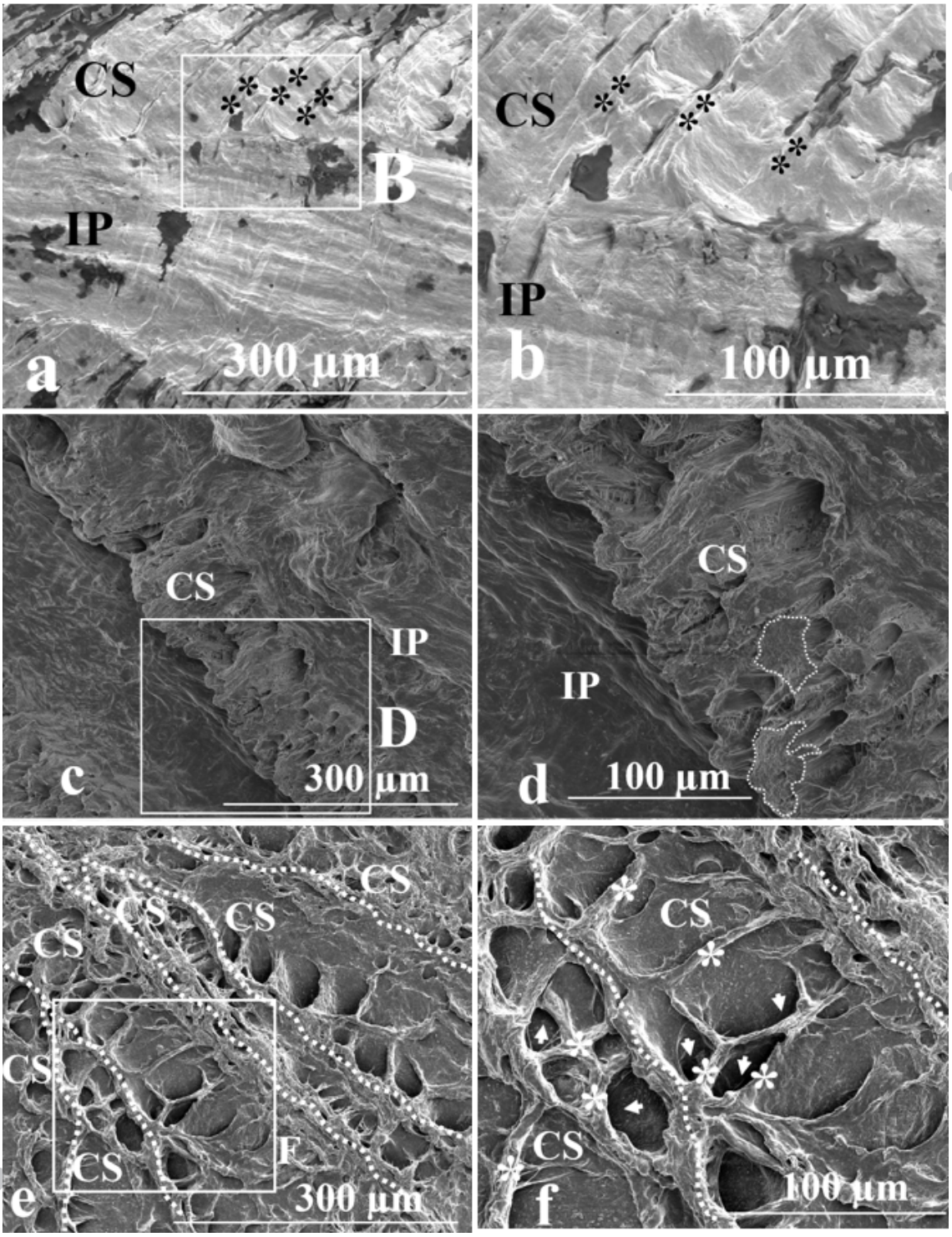

Figure 2. Comparison between control and digested samples. **SEM images of the PBs (some of which are denoted by stars) organization under different magnifications for both control in oblique plane (a 600×, b 1702×), digested (c 492×,d 1126×) and**

additional digestion (e 606×,f 1336×) samples in two different oblique (c, d) and transverse (e, f) cutting planes. Images a, c and e were obtained from different samples. SEM images demonstrate the different organization of PBs in CS and IP lamellae. White dashed lines show collagen bundle cross sections in a CS lamella (d) and boundaries between adjacent CS lamellae (e, f), respectively. B (a), D (c) and F (e) boxes represent magnified regions as shown in b, d and f images, respectively. Arrow heads (f) indicate fenestrae that were created after digestion and removal of matrix.

3.2. Partition boundaries ultrastructure in the transverse plane (0°)

Figure 3 shows SEM images of elastic fibres ultrastructural organization of a PB in a digested sample, spanning six magnification ranges from 160× to 7559×. Elastic fibres within the PB formed a complex and dense network comprised of thick (approximate diameter 1-2 μm) and thin (approximately 0.1 μm in diameter) fibres (Figure 3d-f). Thick elastic fibres within the network were parallel to each other and made an angle relative to the transverse plane, while connecting adjacent lamellae (Figure 3f). It appeared that collagen bundles were enclosed by this network of elastic fibres (Figure 3d, e).

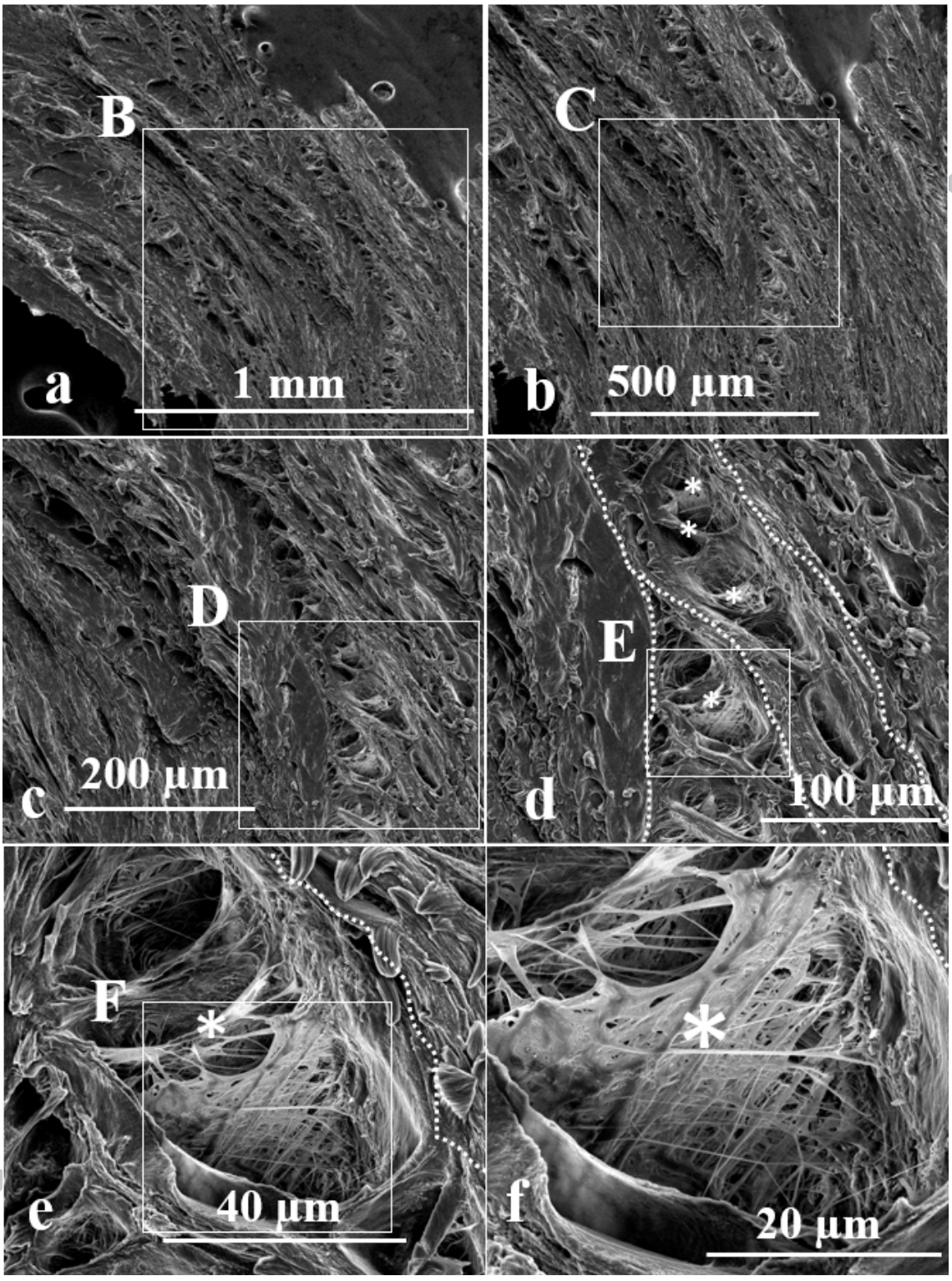

Figure 3. Ultra-structural organization of PB elastic fibres under different magnifications in the transverse (0°) cutting plane. Thick and thin fibres create a network structure. The white boxes denoted by B, C, D, E and F correspond to higher

magnified b, c, d, e and f images, respectively. Magnification factors of SEM images in Figures "a" to "f" were 160×, 275×, 600×, 1166×, 3876× and 7559×, respectively. White dashed lines and stars show boundaries between adjacent CS lamellae and PBs, respectively.

Within the PBs in the transverse plane, the frequently occurring features (dense elastic network with complex structure, different size and shape of elastic fibres) are presented in Figure 4. The dense elastic network was visible after digestion in all samples. The empty spaces, located between the PBs, were collagen bundle cross sections that were removed after digestion.

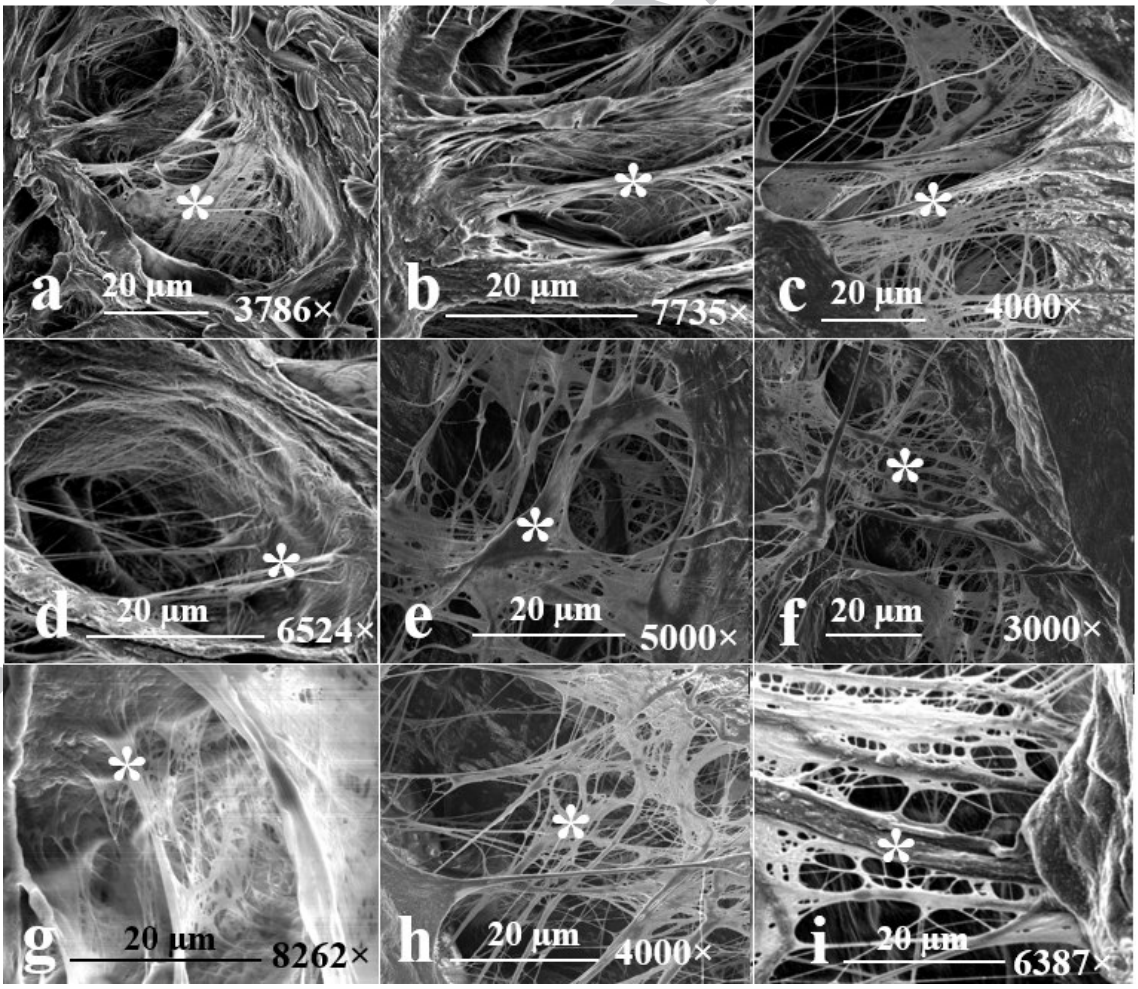

Figure 4. Frequently occurring features of a network comprised of thin and thick elastic fibres across all nine digested samples (transverse plane (0°)) at 20 µm scale bar. Partition boundaries are denoted by stars in all figures.

3.3. Partition boundaries ultrastructure in the oblique plane (30°)

Figure 5 shows SEM images of elastic fibre organization in a selected PB from an oblique cutting plane spanning six magnifications ranging 471× to 14848× (Figures 5a-f) and at four different viewing angles of rotation under 14848× magnification (Figures 5g-j). Elastic fibres within the PB formed a complex network and seemed to connect collagen bundles in a CS lamellae. Under higher magnification (Figures 5e-f), the ultrastructural organization of elastic fibres (denoted by white arrow heads, Figure 5f) in a PB (that was located between two adjacent collagen bundles) was apparent. For better clarification the cross section of two adjacent collagen bundles was identified by white dashed lines and denoted by stars. In Figures 5e-f, the orientation of collagen fibres from adjacent bundles was identified by white arrows, while being interconnected by elastic fibres in the PB.

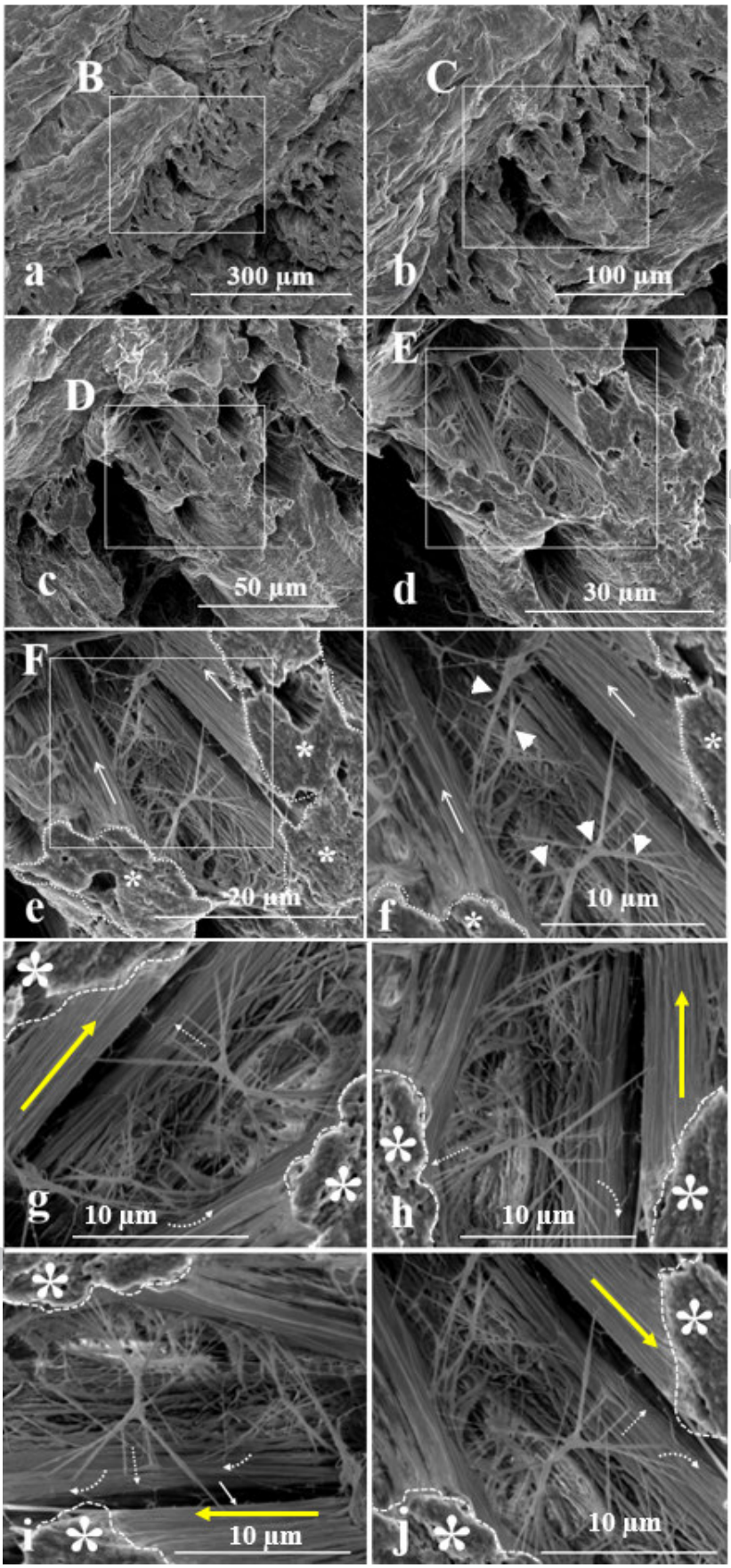
B
a
300 µm
C
b
100 µm
D
c
50 µm
E
d
30 µm
F
e
20 µm
f
10 µm
g
10 µm
h
10 µm
i
10 µm
j
10 µm

Figure 5. SEM images of a cross section (CS) lamella at an oblique cutting plane reveal the elastic fibre ultra-structural organization in one sample under different magnifications (a-f, having magnification factor of 471×, 1126×, 2356×, 5352×, 8534×, 14848×, respectively). The white boxes denoted by B, C, D, E and F correspond to higher magnified b, c, d, e and f images, respectively. Elastic fibres (denoted by white arrow heads) between two adjacent collagen bundles, whose cross sections were surrounded by white dashed lines and denoted by stars (e-f), are shown. Collagen fibres bundles are denoted by white arrows. The elastic network in the same PB (at an oblique cutting plane) shown (yellow arrows) at four different viewing angles of rotation (g-j) under same magnification (14848×). With dashed curved and straight arrows indicate two different possibilities that exist at collagen bundles- PB boundaries. Some elastic fibres merge into the adjacent collagen bundles to be oriented in parallel to the collagen fibres (denoted by curved arrows). While other elastic fibres seem to penetrate directly into the adjacent bundles (denoted by straight arrows).

Four different viewing angles of rotation of a high magnified PB are shown in Figures 5g-j. At the PB-adjacent collagen bundle boundaries, where elastic fibres seem to penetrate into the adjacent bundles, two different kinds of anchoring were observed. Some elastic fibres merged into the adjacent collagen bundles to be oriented in parallel to the collagen fibres (denoted by curved arrows). While other elastic fibres seemed to penetrate directly into the adjacent bundles (denoted by straight arrows).

Similar to the transverse cutting plane, a dense network of thick and thin interconnecting elastic fibres (1.5 to 0.2 µm diameter, respectively) was observed as a key structural feature of PB in the oblique cutting plane across all digested samples at 30° (Figures 6a-i).

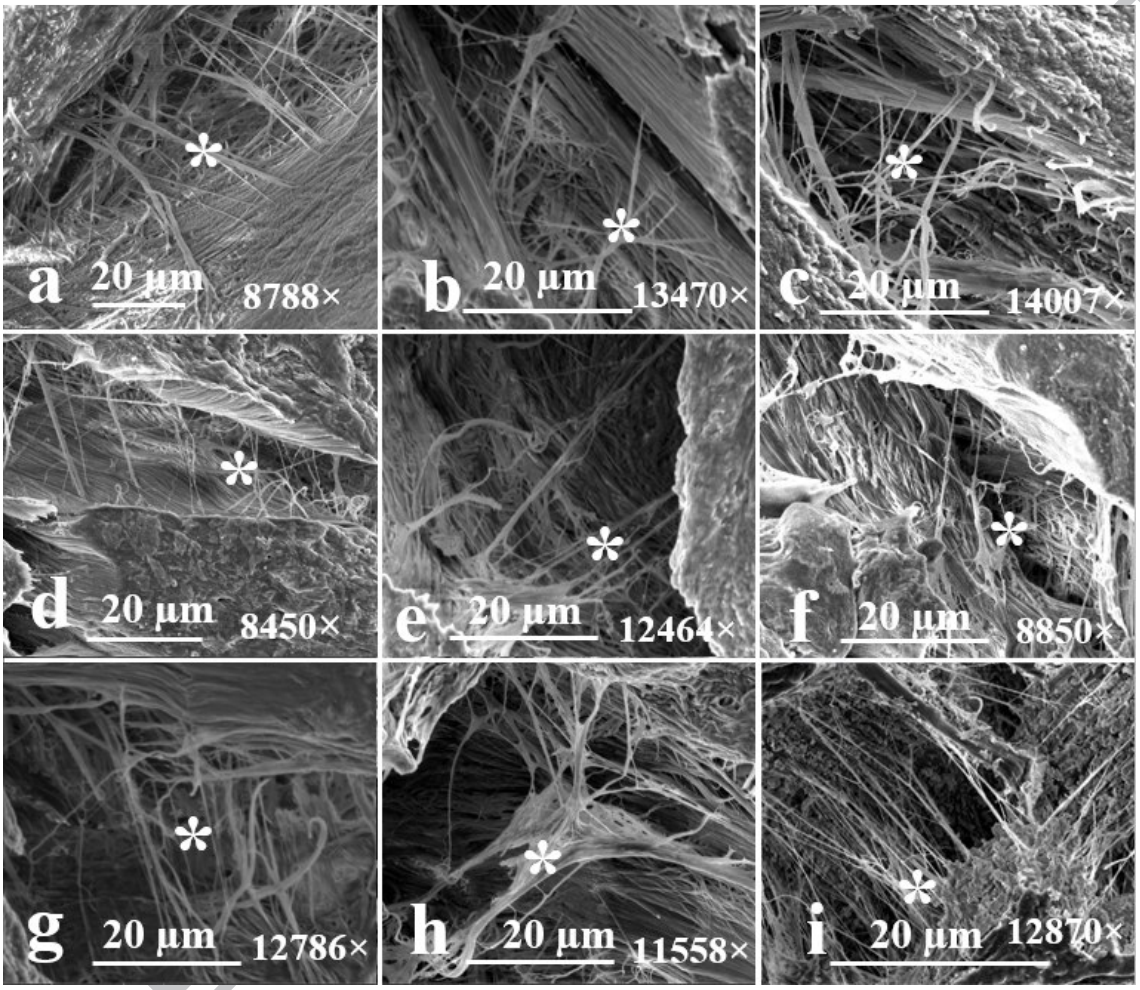

Figure 6. Frequently occurring features of the elastic fibre network (denoted by stars), including thick and thin fibres across all nine digested samples (oblique cutting plane).

3.4. Quantitative analysis

The quantitative analyses (Figures 7a and 7c) show the directional coherency coefficient and the organization of elastic fibres in the PB of digested samples at two different cutting plane

angles (transverse and oblique). The directional coherency coefficient and the orientation of elastic fibres was measured relative to the TCD plane (Figure 7b).

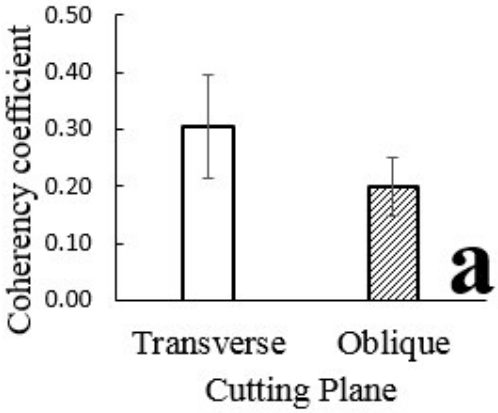
Coherency coefficient
0.50
0.40
0.30
0.20
0.10
0.00
a
Transverse
Oblique
Cutting Plane

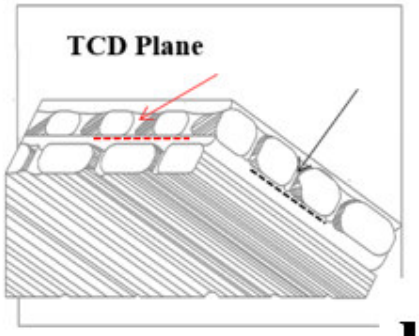
TCD Plane

b

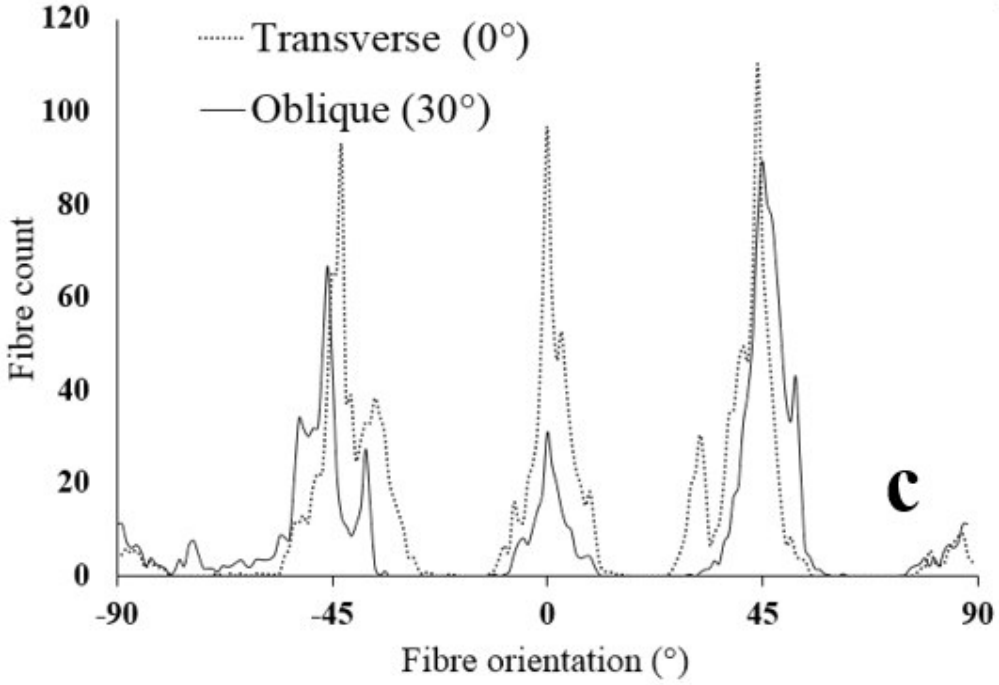
Transverse (0°)
Oblique (30°)
Fibre count
120
100
80
60
40
20
0
-90
-45
0
45
90
Fibre orientation (°)
c

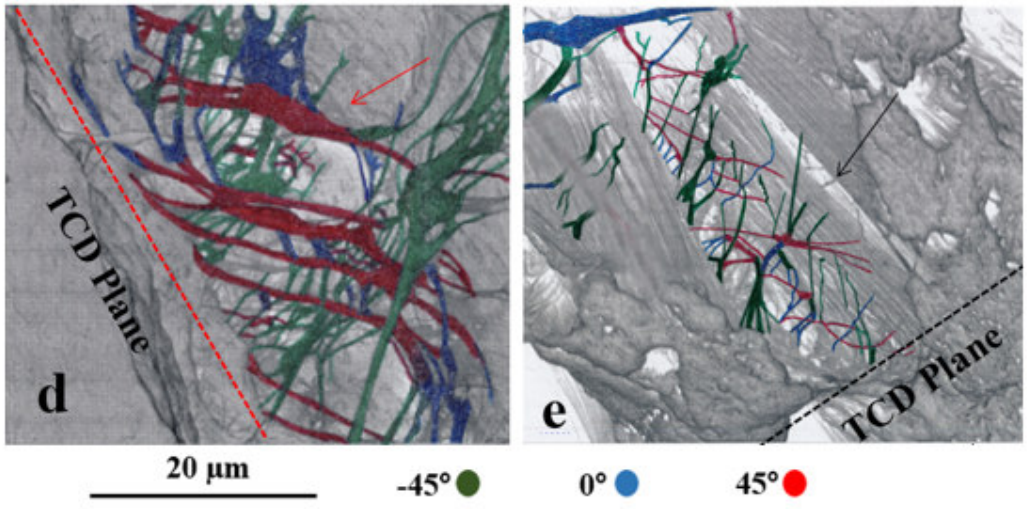
TCD Plane
d
e
TCD Plane
20 µm
-45°
0°
45°

Figure 7. Directional coherency coefficient of elastic fibres in PBs reported as Mean (95% CI) for all digested samples in two different cutting planes (a). Fibre directional coherency coefficient and their orientation were measured relative to the TCD plane (b). Three principal angles of rotation ±45° and 0° (c) were coloured in green, red and blue in inverted images of two PBs at two different cutting angles of 0° (d) and 30° (e), respectively. Red and black arrows show corresponding locations of the PBs indicated in the schematic drawing (b) and SEM images (d-e).

Mean (95%CI) values for directional coherency coefficients of elastic fibres were equal to 0.306 (0.04) and 0.20 (0.03) in the transverse and oblique cutting planes, respectively (Figure 7a). A coherency coefficient close to 1 indicates a strongly coherent orientation of the local fibres, and a value of zero denotes no preferential orientation. There was no significant difference in directional coherency coefficient of elastic fibres between the two different cutting planes ($p = 0.35$). Fibre count-orientation analysis detected principal symmetrically organized angles of rotation (±45°, 0° and ±90°) in both cutting planes (figure 7c).

A geometric 3D presentation of PBs was obtainable based on SEM images in both transverse and oblique cutting planes (Figure 8).

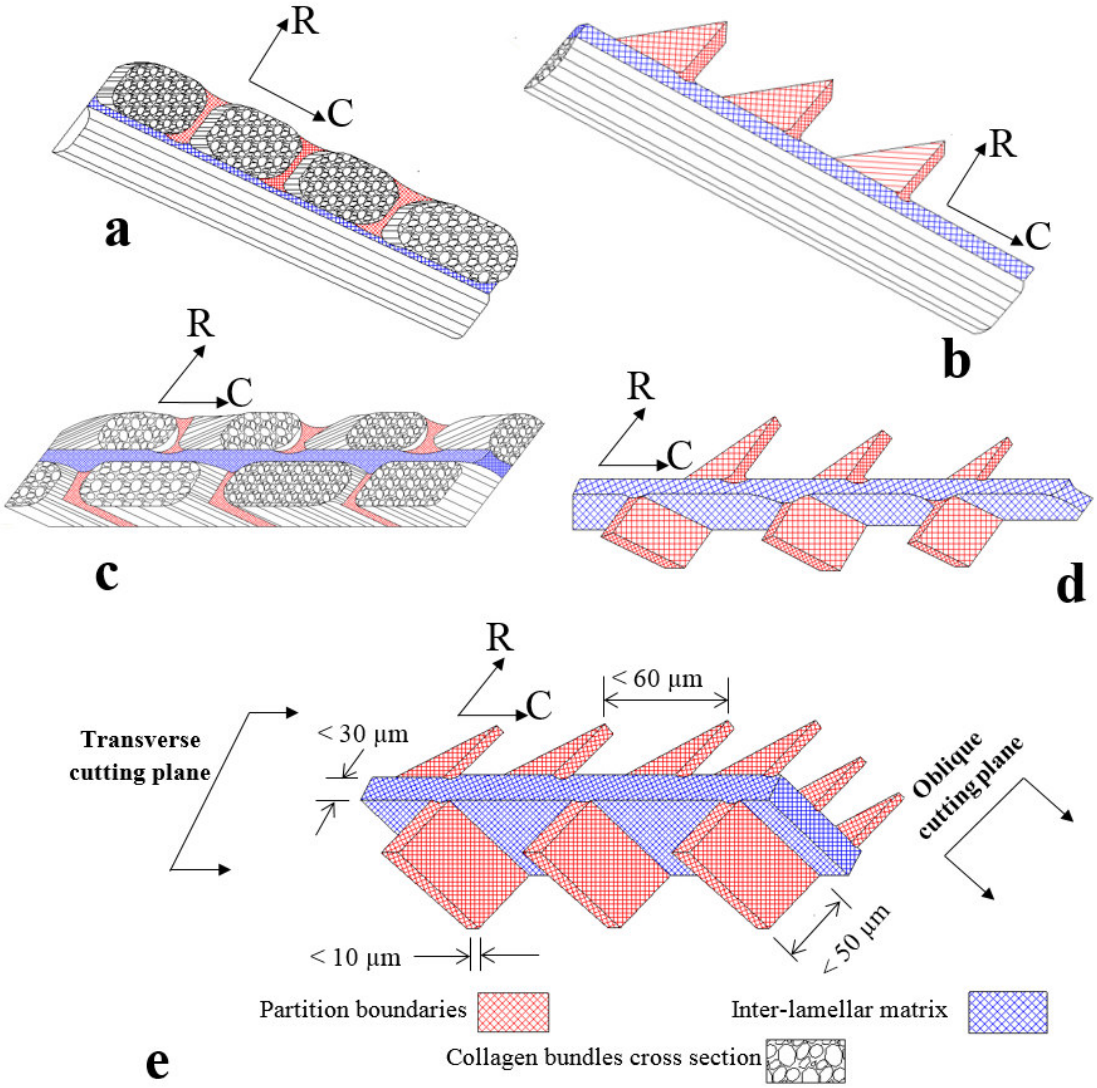

Figure 8. Schematic 3D presentation of PBs in an oblique (a, b) and a transverse cutting plane (c, d) is shown. PBs are in red and the ILM identified in blue. Figures b and c show schematic drawing of PBs after collagen bundles removal from the adjacent lamellae. Geometrical analysis of PBs is presented in panel e. Radial and circumferential directions were denoted by R and c, respectively.

PBs were less than 10 µm thick and their length in the radial direction was less than 50 µm for those PBs that don't completely divide CS lamellae. The length of a complete PB, which

connects two adjacent ILM in radial direction, is approximately 120-150 μm. The distance between two adjacent PBs in a CS lamellae was measured as less than 60 μm, and the ILM thickness was less than 30 μm (Figure 8e).

4. Discussion

The current study was designed to identify the ultrastructural organization of elastic fibres in the PBs, which is an initial and important step toward identification of the mechanical role of elastic fibres in the disc. Referring to our previous studies, where the ultrastructural organization of elastic fibres within the ILM and intra-lamellar region were visualized, it was found that the distribution of elastic fibre orientation was similar in both intra- and inter-lamellar regions. The present study showed that the distribution of elastic fibre orientation was similar to the ILM and intra-lamellar regions. It seems that the organization of elastic fibres in all three regions are similar; however, their function may be different. The presence and arrangement of elastic fibres in PBs were described previously under light microscopy in both cross section (CS) and in-plane (IP) lamellae [33]; however, their ultra-structural organization has not been previously described. Using a technique to remove collagen, proteoglycans and matrix from the AF, while leaving elastic fibres intact [36], the ultrastructural organization of the elastic fibres in the inter- and intra-lamellar regions were successfully described [37]. Utilizing the same technique, current SEM study has described the ultrastructural architecture of the elastic components in the PBs of the AF lamellae.

In spite of using a novel method for visualizing elastic fibres that enabled us to present SEM images of PBs elastic network, there are a few limitations that need to be addressed. An ovine model was used for the current study based on its structural and biochemical similarities to the human disc; however, using human samples are more clinically relevant. The findings of this study may be affected by remnants of undigested matrix or undigested components;

however, only regions where undigested tissue did not obscure elastic fibres were analysed for quantitative analysis. On the other hand, the sample preparation method including digestion, indirect heat treatment and drying, was found to alter the fibre orientation by approximately 2° compared to the control samples [36]. Therefore, it is unlikely that this orientation affects the overall quantitative analysis as it is small in magnitude [41]. Like other SEM studies, identification of elastic fibres by their physical appearance and size is another limitation. Elastic fibres were distinguished from other fibrous components as they are generally twisted or straight strands (0.2-1.5 μm in diameter) that sometimes branch to introduce a course network [42-44]. Further studies will be required to investigate the elastic fibre characteristics in different disc regions (e.g., anterior, lateral and posterolateral) or showing the effect of age, degeneration or disease on elastic fibre ultrastructural organization.

Based on SEM images obtained from transverse cutting planes, the frequent presence of PBs dividing the CS lamellae across the AF (Figures 2a, b, e, f and 3d, e) indicated a well-organized interconnecting structure comprised of elastic fibres. Consistent with other studies, collagen bundles in the CS lamellae of the AF provide a segmental structure that is surrounded by a network of elastic fibres in the PBs and inter-lamellar matrix (Figure 3b) [33-35]. This compartmentalization of the AF by traversing PBs was seen in SEM images in the transverse cutting plane (Figures 2e-f). SEM imaging of a control sample did not reveal elastic fibres in the PBs due to the presence of matrix and collagen constituents, while PBs appear to constitute a constant or definite pattern that recurs at uniform intervals (denoted by stars in Figure 2a-b). As a consequence of partial digestion, a fenestration structure of various sizes was seen to randomly scatter across the CS lamellae (cutting plane = 0°) indicating that PBs are irregularly distributed across the AF (Figures 2e-f). Previously it was believed that PBs divide collagen bundles. However, we have shown that PBs both divide and enclose collagen bundles. This PB arrangement is in agreement with findings that indicated the role

of elastic fibres on AF radial integrity [5, 6]. Also their contribution to enhance disc mechanical properties is unknown.

By removing the matrix and collagen fibres, it is now possible to visualize elastic fibre organization within the PBs, and to our knowledge this new interpretation of elastic fibre ultrastructure has not been previously reported. In both cutting planes (transverse and oblique), a dense network including thick (1-2 μm diameter) and thin (less than 0.2 μm diameter) elastic fibres were seen in the PBs (Figures 3f and 5f).

Analysing the ultrastructural organization of elastic fibres in the PBs in the oblique plane revealed that elastic fibres connect adjacent collagen bundles in a CS lamella by two mechanisms: merging with and becoming orientated in parallel to the collagen fibres; or by a sharp penetration into adjacent collagen bundles (Figures 5g and j). A similar anchoring mechanism was reported within the boundaries between the inter-lamellar matrix and adjacent lamella [37]. Based on the proposed 3D geometrical model of the PB (Figure 8), a possible function of elastic fibres in the PBs is to structurally reinforce adjacent collagen bundles during loading. Could PBs not only enclose collagen fibre bundles, but rather form a branching elastic fibre network between these bundles to provide some form of reinforcement.

Quantitative analysis revealed that there was no significant difference in structural organization of elastic fibres between the transverse and cutting planes. While at least three principle orientations of elastic fibres in the PB were identified, the relatively low magnitudes of coherency coefficients would suggest that the organization of elastic fibres in the PBs represented a more isotropic than anisotropic structure. However, investigations comparing a random network of fibres representing a more isotropic structure, to a preferential fibre orientation that more closely indicates an orthotropic structure with well-organized fibres at 0° and ±45° (Figure 7c), the coherency coefficients were the same. The frequently occurring

features including a dense elastic network, having a complex structure with different size and shape of elastic fibres, were seen across all nine specimens in both cutting planes (Figures 4 and 6).

Based on the presented results the likely mechanical role of PBs in the AF can be speculated, however, a study of the mechanical properties of the PBs is required to provide new mechanical insights, and the current study represents the first steps towards this. The same method that was carefully developed for visualization of the elastic fibre organization in the ILM and lamellae, was utilized to present an ultrastructural understanding of the elastic fibre network in the PBs, which is new knowledge that has not been presented before. Furthermore, with the new proposed 3D geometry of the PBs resulting from the present study (Figure 8), more-accurate multiscale computational models of the disc can be developed, which will provide new insights on the mechanics of the disc.

5. Conclusion

A detailed understanding of the PB ultrastructure is crucial to elucidate its role on the structural integrity of the adjacent collagen bundles, as well as adjacent lamellae. The present study used extracellular matrix digestion to address significant gaps in understanding of disc ultrastructure, and will contribute to multidisciplinary ultrastructure-function studies. The findings presented reveal a well-organized elastic fibre network with a complex ultrastructure that spreads across the PB in both transverse and oblique cutting planes. The present study revealed that a continous network of elastic fibres may provide disc integrity by connecting adjacent bundles of CS lamellae together.

6. References

[1] A.K. Baldwin, A. Simpson, R. Steer, S.A. Cain, C.M. Kielty, Elastic fibres in health and disease, Expert Rev Mol Med 15 (2013) 1-30.

[2] G.S. Montes, Structural biology of the fibres of the collagenous and elastic systems, Cell Biol Int 20(1) (1996) 15-27.

[3] M.D. Humzah, R.W. Soames, Human intervertebral disc: Structure and function, The Anatomical record 220(4) (1988) 337-356.

[4] H. Tseng, K.J. Grande-Allen, Elastic fibers in the aortic valve spongiosa: a fresh perspective on its structure and role in overall tissue function, Acta Biomater 7(5) (2011) 2101-2108.

[5] L.J. Smith, S. Byers, J.J. Costi, N.L. Fazzalari, Elastic fibers enhance the mechanical integrity of the human lumbar anulus fibrosus in the radial direction, Ann Biomed Eng 36(2) (2008) 214-223.

[6] M. Mengoni, B.J. Luxmoore, V.N. Wijayathunga, A.C. Jones, N.D. Broom, R.K. Wilcox, Derivation of inter-lamellar behaviour of the intervertebral disc annulus, J Mech Behav Biomed 48 (2015) 164-172.

[7] C. Vergari, J. Mansfield, J.R. Meakin, P.C. Winlove, Lamellar and fibre bundle mechanics of the annulus fibrosus in bovine intervertebral disc, Acta Biomater 37 (2016) 14-20.

[8] J. Yu, J.C. Fairbank, S. Roberts, J.P. Urban, The elastic fiber network of the anulus fibrosus of the normal and scoliotic human intervertebral disc, Spine 30(16) (2005) 1815-20.

[9] J.P. Urban, S. Roberts, Degeneration of the intervertebral disc, Arthritis research & therapy 5(3) (2003) 120-30.

[10] J.K. Crean, S. Roberts, D.C. Jaffray, S.M. Eisenstein, V.C. Duance, Matrix metalloproteinases in the human intervertebral disc: role in disc degeneration and scoliosis, Spine 22(24) (1997) 2877-84.

[11] R.P. Mecham, T.J. Broekelmann, C.J. Fliszar, S.D. Shapiro, H.G. Welgus, R.M. Senior, Elastin degradation by matrix metalloproteinases. Cleavage site specificity and mechanisms of elastolysis, The Journal of biological chemistry 272(29) (1997) 18071-6.

[12] K. Fujita, T. Nakagawa, K. Hirabayashi, Y. Nagai, Neutral proteinases in human intervertebral disc. Role in degeneration and probable origin, Spine 18(13) (1993) 1766-73.

[13] J.M. Saunders, V.T. Inman, PAthology of the intervertebral disk, Archives of Surgery 40(3) (1940) 389-416.

[14] C. Hirsch, F. Schajowicz, Studies on structural changes in the lumbar annulus fibrosus, Acta Orthop Scand 22(1-4) (1952) 184-231.

[15] J.A. Buckwalter, R.R. Cooper, J.A. Maynard, Elastic fibers in human intervertebral discs, The Journal of Bone & Joint Surgery 58(1) (1976) 73.

[16] D.S. Hickey, D.W. Hukins, Collagen fibril diameters and elastic fibres in the annulus fibrosus of human fetal intervertebral disc, J Anat 133(Pt 3) (1981) 351-7.

[17] E.F. Johnson, H. Berryman, R. Mitchell, W.B. Wood, Elastic fibres in the anulus fibrosus of the adult human lumbar intervertebral disc. A preliminary report, J Anat 143 (1985) 57-63.

[18] J. Sylvest, B. Hentzer, T. Kobayasi, Ultrastructure of prolapsed disc, Acta Orthopaedica Scandinavica 48(1) (1977) 32-40.

[19] F. Postacchini, M. Bellocci, P.T. Ricciardi-Pollini, A. Modesti, An ultrastructural study of recurrent disc herniation: a preliminary report, Spine 7(5) (1982) 492-7.

[20] Y. Mikawa, H. Hamagami, J. Shikata, T. Yamamuro, Elastin in the human intervertebral disk. A histological and biochemical study comparing it with elastin in the human yellow ligament, Archives of orthopaedic and traumatic surgery. Archiv fur orthopadische und Unfall-Chirurgie 105(6) (1986) 343-9.

[21] K. Olczyk, Age-Related-Changes of Elastin Content in Human Intervertebral Disks, Folia Histochem Cyto 32(1) (1994) 41-44.

[22] J.M. Cloyd, D.M. Elliott, Elastin content correlates with human disc degeneration in the anulus fibrosus and nucleus pulposus, Spine 32(17) (2007) 1826-1831.

[23] J. Yu, Elastic tissues of the intervertebral disc, Biochemical Society transactions 30(Pt 6) (2002) 848-52.

[24] J. Yu, C. Peter, S. Roberts, J.P. Urban, Elastic fibre organization in the intervertebral discs of the bovine tail, J Anat 201(6) (2002) 465-475.

[25] C.M. Kielty, M.J. Sherratt, C.A. Shuttleworth, Elastic fibres, J Cell Sci 115(Pt 14) (2002) 2817-28.

[26] J. Yu, U. Tirlapur, J. Fairbank, P. Handford, S. Roberts, C.P. Winlove, Z. Cui, J. Urban, Microfibrils, elastin fibres and collagen fibres in the human intervertebral disc and bovine tail disc, J Anat 210(4) (2007) 460-471.

[27] L.J. Smith, N.L. Fazzalari, Regional variations in the density and arrangement of elastic fibres in the anulus fibrosus of the human lumbar disc, J Anat 209(3) (2006) 359-367.

[28] L.J. Smith, N.L. Fazzalari, The elastic fibre network of the human lumbar anulus fibrosus: architecture, mechanical function and potential role in the progression of intervertebral disc degeneration, Eur Spine J 18(4) (2009) 439-48.

[29] J.T. Martin, A.H. Milby, J.A. Chiaro, D.H. Kim, N.M. Hebela, L.J. Smith, D.M. Elliott, R.L. Mauck, Translation of an engineered nanofibrous disc-like angle-ply structure for intervertebral disc replacement in a small animal model, Acta Biomater 10(6) (2014) 2473-2481.

[30] E.F. Johnson, K. Chetty, I.M. Moore, A. Stewart, W. Jones, The distribution and arrangement of elastic fibres in the intervertebral disc of the adult human, J Anat 135(Pt 2) (1982) 301-9.

[31] E.F. Johnson, R.W. Caldwell, H.E. Berryman, A. Miller, K. Chetty, Elastic fibers in the anulus fibrosus of the dog intervertebral disc, Acta anatomica 118(4) (1984) 238-42.

[32] J. Tavakoli, D.M. Elliott, J.J. Costi, Structure and mechanical function of the inter-lamellar matrix of the annulus fibrosus in the disc, Journal of orthopaedic research : official publication of the Orthopaedic Research Society 34(8) (2016) 1307-15.

[33] J. Yu, M.L. Schollum, K.R. Wade, N.D. Broom, J.P. Urban, ISSLS Prize Winner: A Detailed Examination of the Elastic Network Leads to a New Understanding of Annulus Fibrosus Organization, Spine 40(15) (2015) 1149-57.

[34] C.A. Pezowicz, P.A. Robertson, N.D. Broom, The structural basis of interlamellar cohesion in the intervertebral disc wall, J Anat 208(3) (2006) 317-330.

[35] M.L. Schollum, P.A. Robertson, N.D. Broom, A microstructural investigation of intervertebral disc lamellar connectivity: detailed analysis of the translamellar bridges, J Anat 214(6) (2009) 805-816.

[36] J. Tavakoli, J.J. Costi, Development of a rapid matrix digestion technique for ultrastructural analysis of elastic fibers in the intervertebral disc, J Mech Behav Biomed 71 (2017) 175-183.

[37] J. Tavakoli, D.M. Elliott, J.J. Costi, The ultra-structural organization of the elastic network in the intra- and inter-lamellar matrix of the intervertebral disc, Acta Biomater 58 (2017) 269-277.

[38] R. Rezakhaniha, A. Agianniotis, J.T. Schrauwen, A. Griffa, D. Sage, C.V. Bouten, F.N. van de Vosse, M. Unser, N. Stergiopulos, Experimental investigation of collagen waviness and orientation in the arterial adventitia using confocal laser scanning microscopy, Biomech Model Mechanobiol 11(3-4) (2012) 461-73.

[39] E. Fonck, G.G. Feigl, J. Fasel, D. Sage, M. Unser, D.A. Rufenacht, N. Stergiopulos, Effect of aging on elastin functionality in human cerebral arteries, Stroke 40(7) (2009) 2552-6.

[40] T.K. Koo, M.Y. Li, A Guideline of Selecting and Reporting Intraclass Correlation Coefficients for Reliability Research, Journal of Chiropractic Medicine 15(2) (2016) 155-163.

[41] R.S. Crissman, L.A. Pakulski, A Rapid Digestive Technique to Expose Networks of Vascular Elastic Fibers for Sem Observation, Stain Technol 59(3) (1984) 171-180.

[42] T. Ushiki, Collagen fibers, reticular fibers and elastic fibers. A comprehensive understanding from a morphological viewpoint, Archives of histology and cytology 65(2) (2002) 109-126.

[43] R.S. Crissman, SEM observations of the elastic networks in canine femoral artery, The American journal of anatomy 175(4) (1986) 481-92.

[44] R.S. Crissman, W. Guilford, The three-dimensional architecture of the elastic-fiber network in canine hepatic portal system, The American journal of anatomy 171(4) (1984) 401-13.

Statement of significance

A detailed ultrastructural study in the partition boundaries of the annulus fibrouses within the disc revealed a well-organized elastic fibre network with a complex ultrastructure. The continous network of elastic fibres may provide disc integrity by connecting adjacent bundles of cross section lamellae together. The density of the elastic fibre network in PBs was lower, and fibre orientation was similar to the intra-lamellar space and the inter-lamellar matrix.